mond deposition is verified experimentally. The most effective reaction on diamond deposition is the next problem.

This was, in part, Paper 1673, presented at the Paris, France, Meeting of the Society, August 31-September 5, 1997.

Manuscript received October 9, 1997.

Aoyama Gakuin University assisted in meeting the publication costs of this article.

REFERENCES

1. C. Pan, C. J. Chu, J. L. Margrave, and R. H. Hauge, *J. Electrochem. Soc.*, **141**, 3246 (1994).
2. N. J. Komplin, B. J. Bai, C. J. Chu, J. L. Margrave, and R. H. Hauge, *Diamond Materials*, J. P. Dismukes and K. U. Ravi, Editors, PV 93-17, p. 385, The Electrochemical Society Proceedings Series (1993).
3. C. Pan, J. L. Margrave, and R. H. Hauge, *Mater. Res. Soc. Symp. Proc.*, **349**, 427 (1995).
4. T. Ando, Y. Yamamoto, S. Suehara, M. Kamo, Y. Sato, S. Shimosaki, and M. N. Gamo, *J. Chin. Chem. Soc.*, **42**, 285 (1995).
5. A. Freedman, *J. Appl. Phys.*, **75**, 3112 (1994).
6. F. C. N. Hong, C. T. Liang, J. J. Wu, D. Chang, and J. C. Hsieh, *Appl. Phys. Lett.*, **63**, 3149 (1993).
7. F. C. N. Hong, J. C. Hsieh, J. J. Wu, G. T. Lian, and J. H. Hwang, *Diamond Relat. Mater.*, **2**, 365 (1993).
8. C. H. Chu and M. H. Hon, *Diamond Relat. Mater.*, **2**, 311 (1993).
9. T. Nagano and N. Shibata, *Jpn. J. Appl. Phys.*, **32**, 5067 (1993).
10. P. K. Bachmann, H. J. Hagemann, H. Lade, D. Leers, F. Pitch, D. U. Wiechert, and H. Wilson, *Mater. Res. Soc. Symp. Proc.*, **339**, 267 (1995).
11. T. Kotaki, N. Horii, H. Isono, and O. Matsumoto, *J. Electrochem. Soc.*, **143**, 2003 (1996).
12. N. Horii, N. Suzuki, K. Itoh, T. Kotaki, and O. Matsumoto, *Diamond Relat. Mater.*, **6**, 1874 (1997).
13. R. S. Tsang, C. A. Rego, P. W. May, J. Thumin, M. N. R. Ashfold, K. N. Rosser, C. M. Younes, and M. J. Holt, *Diamond Relat. Mater.*, **5**, 359 (1996).
14. B. J. Bai, C. J. Chu, D. E. Patterson, R. H. Hauge, and J. L. Margrave, *J. Mater. Res.*, **8**, 233 (1993).
15. T. Kotaki, Y. Amada, K. Harada, H. Uyama, and O. Matsumoto, *Diamond Relat. Mater.*, **2**, 342 (1993).
16. I. Schmidt, F. Hentschel, and C. Benndorf, *Diamond Relat. Mater.*, **5**, 1318 (1996).

Microcrystalline Silicon Film Deposition from H_2-He-SiH_4 Using Remote Plasma Enhanced Chemical Vapor Deposition

Sung-Woo Lee,[a] Du-Chang Heo, Jin-Kyu Kang, Young-Bae Park,[b] and Shi-Woo Rhee*

Laboratory for Advanced Materials Processing, Department of Chemical Engineering, Pohang University of Science and Technology, 790-784 Pohang, Korea

ABSTRACT

Microcrystalline silicon (μc-Si:H) films were deposited at 250°C from the reaction of SiH_4 with H_2-He gas excited in an inductively couple remote plasma. The deposition rate, microstructure, and material properties of μc-Si:H depended on the composition of hydrogen and helium in the plasma. Si films deposited on a hydrogen plasma showed columnar and microcrystalline structure with a grain size of about 200 Å or less, and had an optical bandgap of about 2.05 to 2.1 eV. The microstructure parameter (SiH_2/[SiH + SiH_2] in the film) and Urbach tail slope decreased with increasing H_2 fraction in the plasma gas. On the other hand, amorphous (a-Si:H) film was deposited with higher deposition rate when pure He was used as plasma gas and the optical bandgap of this film was 2.18 eV. The surface of a-Si:H film was smoother than that of μc-Si:H.

Introduction

Amorphous, microcrystalline (a-, μc-Si:H), and polycrystalline silicon films have been used in many devices such as thin film transistors (TFTs) and solar cells. In the field of active matrix liquid crystal displays (AMLCDs), the use of poly-Si as an active layer instead of a-Si has attracted much attention because the electron mobility in poly-Si is much higher than that of a-Si and a better performance can be achieved with poly-Si TFT.[1-5] Because of the high uniformity of the small grain size, μc-Si has some attractive electrical properties. The high mobility of μc-Si, in particular, is strongly expected to enable realization of high speed devices on glass substrates.[3,6,7] Also, due to its more rigid structure, μc-Si may be a solution to one significant problem with a-Si:H, its instability.[8]

The deposition of μc-Si and poly-Si films by plasma enhanced chemical vapor deposition (PECVD), photochemical vapor deposition, and hot-filament chemical vapor deposition has been extensively studied and several controversial crystallization mechanisms have been proposed[9-14]: (*i*) enhancement of the adsorbed radical (such as SiHx [x = 2 or 3]) diffusion by hydrogen on the surface, (*ii*) preferential etching of weak and strained amorphous Si–Si bonding by atomic hydrogen, and (*iii*) chemical annealing by atomic hydrogen in the growth zone. Thereby, it is important to supply sufficient atomic hydrogen to deposit crystalline Si. It is well known that the surface of films is roughened by the hydrogen plasma.[15]

Wang et al. have reported that polycrystalline Si films were deposited at 250°C, using a hydrogen dilution method with electron cyclotron resonance (ECR) plasma CVD.[16] The deposition rate was critically dependent on the H_2/(H_2 + SiH_4) ratio; above 92%, crystallinity could be obtained. Their results also showed the important role of atomic hydrogen for poly-Si deposition. SiH_4-H_2 mixtures are most popular and also various diluent and plasma gases such as He, Ar, Ne, Kr, and Xe have been used to deposit Si films.[17-22] These inert gases lead to the penning ionization process which increases the deposition rate but crystallinity of the film is less than that deposited with excess H_2. It is well known that ion bombardment deteriorates crystallinity. The presence of inert gas in the gas flow destroyed any ordered growth during deposition.[23]

In this study, we have investigated the effect of H_2 and He plasma gases on the film structure and optical properties. Inductively coupled remote plasma was used to generate the activated species, and the deposition was carried out at the downstream of the plasma to reduce the ion bombardment effect. The compositional, optical, and structural properties of the deposited-Si films were characterized by Fourier transform infrared spectroscopy (FTIR), UV-visible spectroscopy, Raman spectroscopy, X-ray diffractometer (XRD), cross-sectional transmission electron microscopy (XTEM), and atomic force microscopy (AFM).

* Electrochemical Society Active Member.
[a] Present address: Samsung Petrochemical Co. Ltd., Ulsan Korea.
[b] Present address: Samsung Electronics Co. Lts., Kiheung, Korea.

Experimental

Film preparation.—In a remote plasma enhanced CVD reactor, H_2 and He gases were introduced into a high purity alumina tube, excited by the inductively coupled radio frequency (rf) (13.56 MHz) plasma, and flowed into the deposition zone. SiH_4 (99.99%) was introduced into the region 10 cm downstream of the plasma and mixed with excited H_2 (99.9999%) and He (99.9999%), and flowed toward the substrate located at 20 cm downstream of the plasma. Thermally oxidized silicon wafer (SiO_2 thickness = 1000 Å), Si(111) wafer, and Corning 7059 glass were used as substrates. For the Si deposition, the reactor pressure was 0.3 Torr, deposition temperature was 250°C, plasma power was 150 W, H_2 and He flow rate ratio (H_2/[H_2 + He]) was in the range of 0 to 100%. Plasma gas flow rate and SiH_4 flow rate were 100 and 10 standard cubic centimeters per minute (sccm), respectively.

Film characterization.—The deposited films were characterized by Midac 1600 FTIR with a liquid nitrogen-cooled HgCdTe (MCT) detector for chemical composition, hydrogen concentration, and its configuration. UV-visible (UV-vis) spectroscopy was used for optical properties such as absorption coefficient (α), optical bandgap (E_g), and Urbach tail slope energy (E_o). Surface roughness and morphology of deposited Si films were observed by Park Science Instrument (PSI) AFM. Root mean square (rms) values of surface roughness were obtained by averaging for three different areas. Structure of the deposited films was analyzed by Rigaku D-MAX 1400 X-ray diffractometer with Cu Kα radiation operating at 50 kV, 150 mA. Raman spectroscopy was also used to examine the film crystallinity using double SPEX monochromator in the spectra range of 200 to 600 cm^{-1}. Resolution was 0.5 cm^{-1} and exciting Ar ion laser power was 200 mW with the wavelength of 5145 Å. The cross section of deposited films was observed by JEOL JEM-4000FX TEM. Cross-sectional specimens for TEM were first glued face to face, cut, then ground, dimpled, and thinned by ion milling. TEM observations were conducted operating at 400 kV.

Results and Discussion

Deposition kinetics.—Figure 1 shows the deposition rate as a function of the H_2 fraction in the plasma (H_2/[H_2 + He]). An increases in the H_2 fraction leads to a decrease in the deposition rate. When the H_2 fraction is 20% or higher, the deposition rate decreased down to 20 Å/min. It indicates that physical collision process such as penning ionization is more dominant in a He plasma because He atoms can be excited into metastable states. There are two metastable states ($^3S_1$ = 19.8 eV, $^1S_0$ = 20.6 eV) and these metastable atoms subsequently pass their excitation energy to the SiH_4 molecule. It seems that He plasma is more efficient in dissociating SiH_4 in the gas phase by physical collision.[24] Moreover hydrogen atoms work as an etchant during film growth.[25] Hydrogen in the plasma induces the change in the morphology of the film from a pure amorphous phase to a mixed amorphous and crystalline phase. There are two regimes in the Si film deposition depending on the balance between deposition and etching. The former produces the disordered network, while the later yields μc-Si or poly-Si even on amorphous substrates such as glass and SiO_2 and epitaxial Si on a single-crystal Si substrate. At high deposition rate, it is more likely that a-Si:H is formed. On the other hand at low deposition rate with hydrogen, the crystallinity of Si:H is increased.

Structure and crystallinity.—Figure 2 shows XRD spectra of the Si film as a function of the plasma gas composition. The deposited-Si films showed both amorphous and crystalline characters depending on the plasma gas composition. Films deposited with pure He plasma showed amorphous structure. The polycrystalline phase appeared in the film at H_2/(H_2 + He) of 20% or higher with the diffraction peaks attributed to the different planes (111), (220), and (311) in the XRD spectra. It indicates that the supply of atomic hydrogen is essential to form μc-Si film.

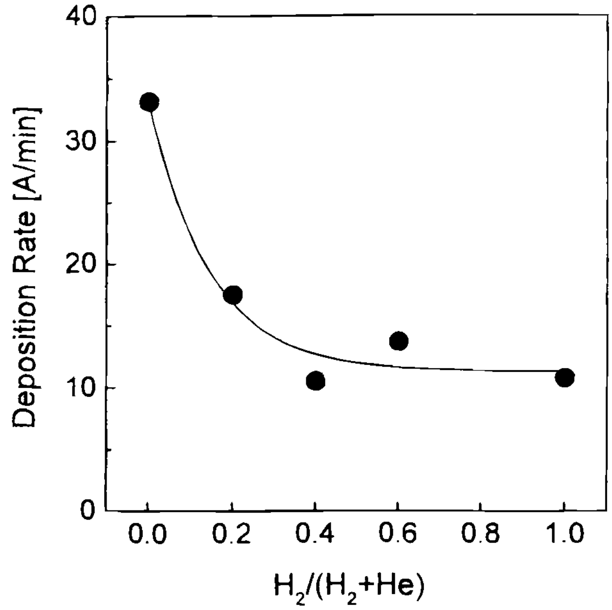

Fig. 1. Deposition rate change as a function of the H_2 fraction in the plasma gas. Temperature, 250°C; pressure, 0.3 Torr; plasma power, 150 W; plasma gas flow rate, 100 sccm; and SiH_4, 10 sccm.

In the presence of a reactive hydrogen plasma, the disordered material will be selectively etched out and the property of ordered material will increase to form μc-Si film.[26] Figure 3 shows the correlation between the grain size of the deposited film and the composition of the plasma gas. The grain size of the deposited film was calculated with Scherrer's formula[27]

$$t = \frac{0.9\lambda}{B\cos\theta} \qquad [1]$$

where t is the average grain size, λ is the X-ray wavelength, B is the full width at half maximum, and θ is the Bragg angle. In case of the pure He plasma gas, the deposited film was amorphous. Even with the small amount of H_2 in the

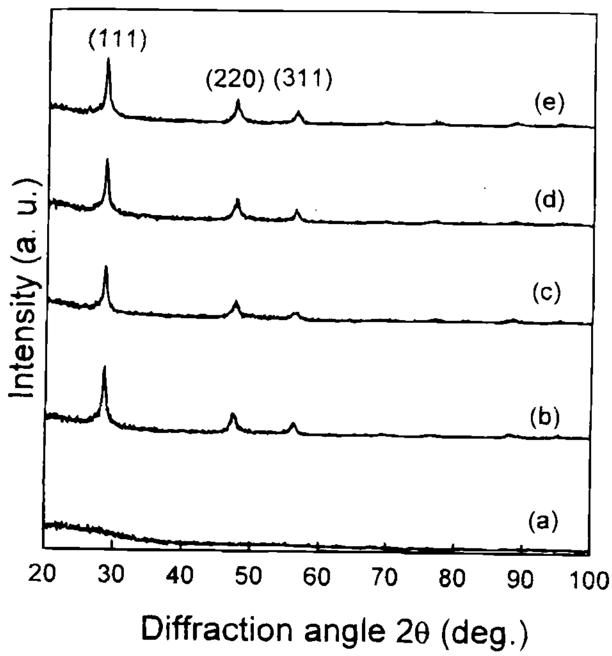

Fig. 2. XRD spectra as a function of the H_2 fraction in the plasma gas. Temperature, 250°C; pressure, 0.3 Torr; plasma power, 150 W; plasma gas flow rate, 100 sccm; and SiH_4, 10 sccm. H_2/(H_2 + He): (a) 0, (b) 0.2, (c) 0.4, (d) 0.6, (e) 1.0.

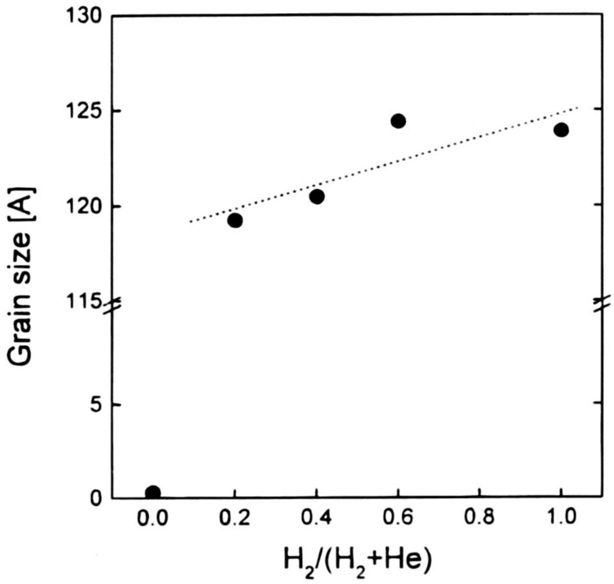

Fig. 3. The grain size of the deposited Si films as a function of the H_2 fraction in the plasma gas. Temperature, 250°C; pressure, 0.3 Torr; plasma power, 150 W; plasma gas flow rate, 100 sccm; and SiH_4, 10 sccm.

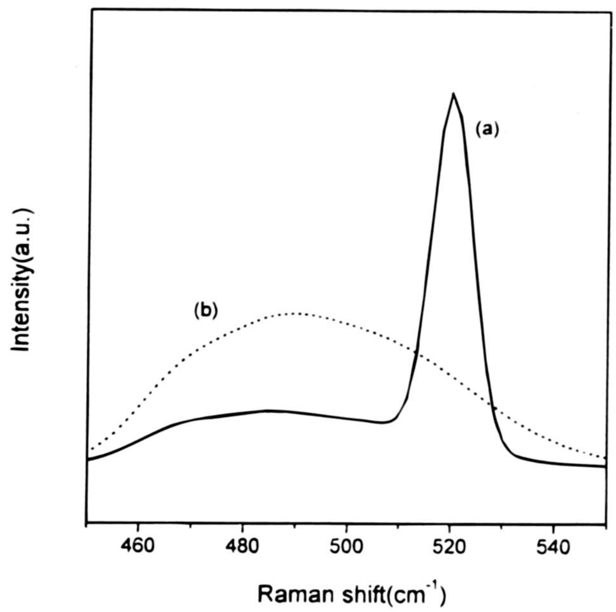

Fig. 4. Raman spectra of the deposited films with (a) pure H_2 plasma gas, and (b) pure He plasma gas. Temperature, 250°C; pressure, 0.3 Torr; plasma power, 150 W; plasma gas flow rate, 100 sccm; and SiH_4, 10 sccm.

plasma, the deposited film showed microcrystalline phase. As the H_2 fraction of the plasma gas was increased, the grain size was increased. It is believed that the increase of the hydrogen coverage on the growing surface enhances the surface diffusion of absorbed radicals, which leads to the increase of the grain size.[28]

Figure 4 shows the difference in Raman spectra between amorphous film deposited with pure He as a plasma gas, and microcrystalline film which was deposited with pure H_2 as a plasma gas. For amorphous Si film, a broad band peak appears around 480 cm^{-1}. For crystalline Si, a sharp peak appears around 520 cm^{-1} with narrow full width at half maximum (FWHM) as the crystallinity increases. Under H_2 plasma, FWHM was about 8.75 cm^{-1}, compared with that of bulk crystalline Si, about 3.5 cm^{-1}. The deposited film under He plasma was fully amorphous.

Figure 5 shows the cross-sectional TEM image and selected area diffraction (SAD) pattern for μc-Si film deposited by pure H_2 plasma. It clearly shows that the deposited Si film has the columnar structure growing in a direction perpendicular to the substrate. The film was made up of a very small needle-like grains approximately 200 Å from the dark field image (Fig. 5b), and those are uniformly distributed in the thickness of the film. The concentric circles of the SAD patterns (Fig. 5c) indicate that the silicon film is polycrystalline. By XRD, Raman, and TEM results, silicon films deposited with H_2 plasma gas were found to have a polycrystalline phase.

Surface morphology.—Figure 6 shows a three-dimensional AFM image of deposited Si films. Surface roughness is affected by the formation of the crystalline phase. The rms of surface roughness is 79 Å for the film deposited with pure He (Fig. 6a) and above 100 Å with He and H_2 mixture (Fig. 6b, c). When H_2 was added in the plasma gas, the roughness of the film was increased with increased H_2 fraction. It is believed that the improvement of the crystallinity increases the surface roughness of the film.

Optical properties.—The optical bandgap is obtained by Tauc's semiempirical equation[29]

$$(\alpha h\nu)^{1/2} = B(h\nu - E_g) \qquad [2]$$

where α is the absorption coefficient, $h\nu$ is the photon energy, E_g is the energy of the optical bandgap, and B is a constant. From the extrapolation of linear regime in the Tauc plot, we can obtain the optical bandgap. It was found that the optical bandgap was 2.05 to 2.1 eV for the film deposited with H_2 plasma, and 2.18 eV with He plasma, respectively.

Optical absorption of the Si films in the UV-visible regions depend on the element of Si and hydrogen in the film network, especially on the number of Si–Si, Si–H bonds, and microvoids in the film.[30] Since the strength of Si–H bonds is stronger than that of Si–Si bonds, the energy separation of bonding and antibonding orbitals of Si–H

Fig. 5. (a) Cross-sectional TEM image of μc-Si:H deposited with pure H_2 plasma (b) dark field image of (a), and (c) SAD pattern.

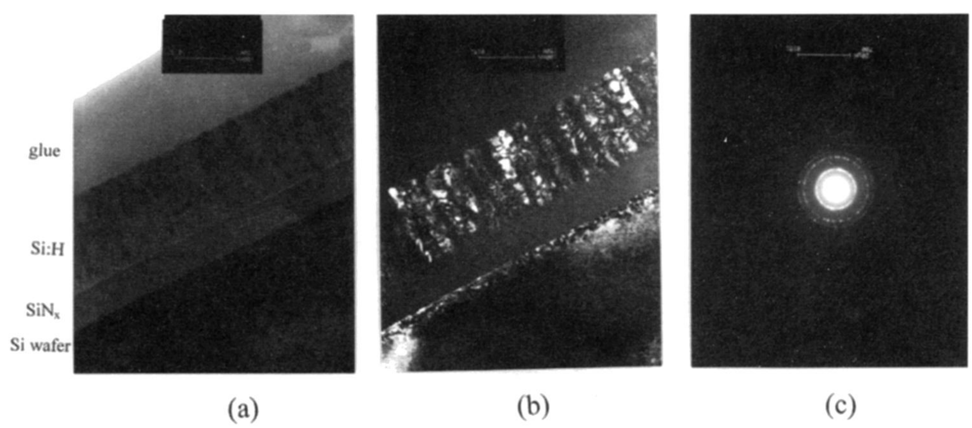

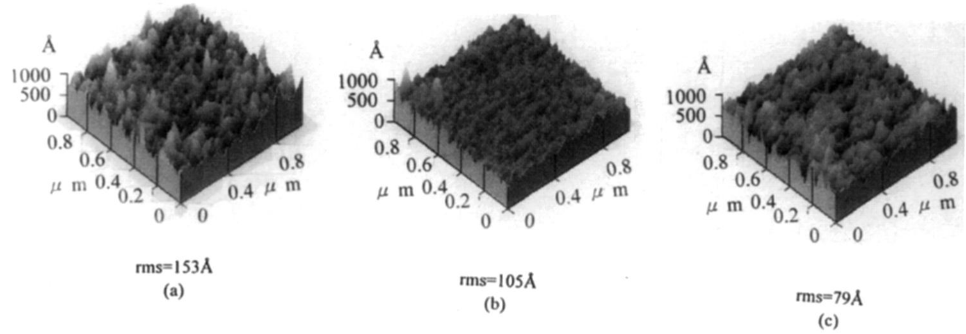

Fig. 6. Three-dimensional AFM images of the Si films. Temperature, 250°C; pressure, 0.3 Torr; plasma power, 150 W; SiH_4, 10 sccm. Plasma gas flow rate, 100 sccm; and $H_2/(H_2 + He)$: (a) 1, (b) 0.6, and (c) 0.

bonds is greater than that of Si–Si bonds. And it has been reported that the bandgap of a-Si:H film increases as the hydrogen content in the film increases.[31] Figure 7 shows that the film deposited with pure He showed largest optical bandgap with highest amount of hydrogen in the film. It was also reported that the film deposited with He plasma showed amorphous structure which had larger optical bandgap than that of crystalline film.[3] Hydrogen content in the film tends to be higher with high deposition rate. Optical bandgap of the film was increased with the increases of H_2 fraction in the plasma because the hydrogen content in the film increases.

Figure 8 shows FTIR silicon-hydrogen bond stretching peaks in the silicon film. The peaks at 1800 to 2300 cm^{-1} represent the bond configurations of monohydride (Si–H), dihydride ($Si–H_2$) and polyhydride [$(SiH_2)_n$].[32] The bonding configurations of SiH and SiH_2 are terminal ($H–Si{\equiv}Si_3$), and bridge ($H_2{=}Si{=}Si_2$) sites, respectively. The microstructure parameter, defined as

$$R = \frac{\int I_{2090}}{\int I_{2090} + \int I_{2000}} \quad [3]$$

is the ratio of the integrated area of the IR mode centered at 2090 cm^{-1} to the IR mode at 2090 and 2000 cm^{-1}. This was examined in order to identify the silicon hydrogen complexes (SiH and SiH_2) in the silicon network structure.

The R parameter represents not only the short range structure but also the long range structure which is related to the inhomogeneities such as voids or agglomerations of voids, and the film porosity. The dense film mainly shows the absorption band at 2000 cm^{-1} (Si–H), while the contribution of the 2090 cm^{-1} mode indicates the presence of SiH_2 in the porous network.[33] In the Si film deposited with pure He as a plasma gas, most of the hydrogen existed in the form of SiH_2 configuration (Fig. 8b). The fraction of Si–H configuration in the film was increased with the increase of hydrogen in the plasma (Fig. 8a).

Figure 9 shows the microstructure parameter R, Urbach tail slope energy E_o, and both changes with H_2 fraction in the plasma gas. E_o represents the slope of the exponential tail from UV-vis spectra. This region has been attributed to

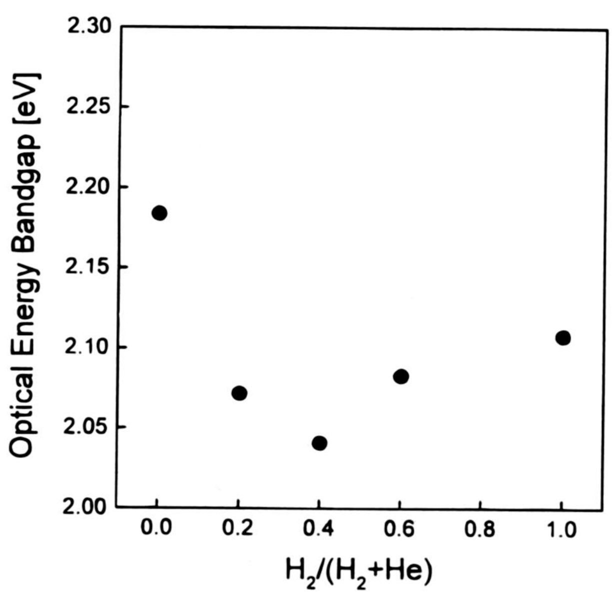

Fig. 7. Optical energy bandgap and hydrogen content of the film as a function of the H_2 fraction in the plasma gas. Temperature, 250°C; pressure, 0.3 Torr; plasma power, 150 W; plasma gas flow rate, 100 sccm; and SiH_4, 10 sccm.

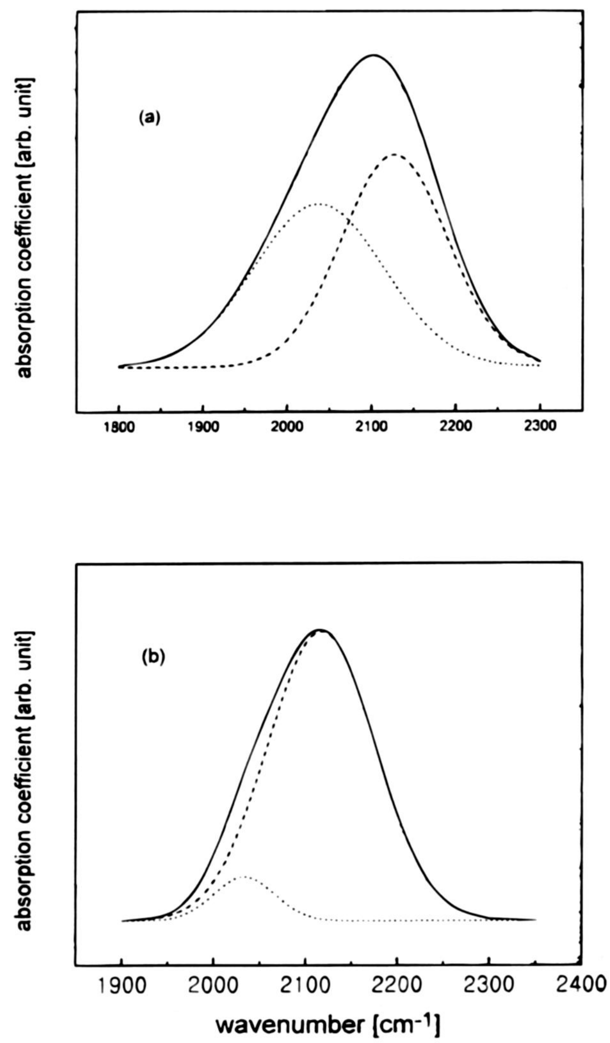

Fig. 8. FTIR spectra of the Si films deposited with (a) pure H_2 plasma gas and (b) pure He plasma gas. Temperature, 250°C; pressure, 0.3 Torr; plasma power, 150 W; plasma gas flow rate, 100 sccm; and SiH_4, 10 sccm.

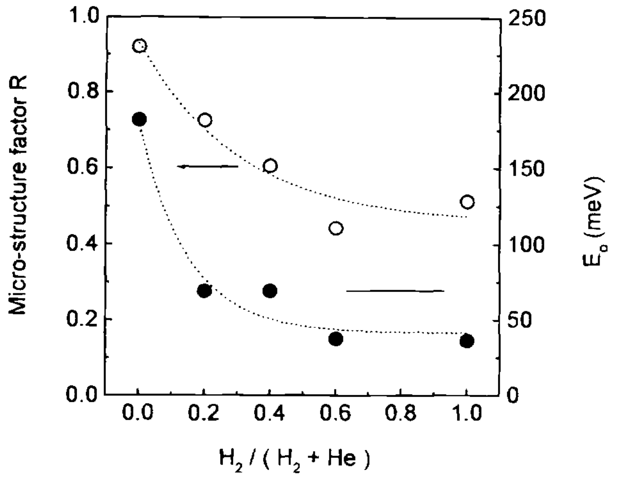

Fig. 9. Microstructure factor from FTIR spectra and Urbach tail slope from UV-vis spectra as a function of the H_2 fraction in the plasma gas. Temperature, 250°C; pressure, 0.3 Torr; plasma power, 150 W; plasma gas flow rate, 100 sccm; and SiH_4, 10 sccm.

an exponential tail of the valence or conduction band, and reflects the randomness of an amorphous network.[34,35] Figure 9 shows that the randomness in the films is related with silicon-hydrogen bonding configuration in the film. R and E_o are decreased with the increase of H_2 fraction in the plasma. It is believed that hydrogen atoms on the growing surface etches out random Si–H_2 and forms Si–H bonding configuration which makes dense network structure in the film. It reduces the bonding angle fluctuation and the stress which makes the tail state width in the bandgap narrow.

Conclusion

We have deposited the a-Si:H and μc-Si:H films by remote H_2 and He plasma gas mixtures and investigated the film composition, hydrogen bonding configuration, optical property, roughness, and structure. The dense and crystalline structure can be obtained with increasing the H_2 fraction in the plasma gas. With helium as a plasma gas, amorphous films (a-Si:H) were deposited with SiH_2 bonding configurations and microscopically disordered and loose networks. Optical bandgap was 2.18 eV. On the other hand, with hydrogen plasma gas, μc-Si were deposited with SiH bonding configurations and relatively dense network. Optical bandgap was about 2.05 to 2.10 eV. The deposition rate with He plasma process is higher than that with H_2 plasma, and amorphous silicon surface is smoother than microcrystalline silicon.

Acknowledgment

This research was supported by Samsung Electronics Company. The authors would like to thank J-H. Hong of RIST, Korea, for his technical support with AFM measurement.

Manuscript submitted May 8, 1997; revised manuscript received April 15, 1998.

Pohang University of Science and Technology assisted in meeting the publication costs of this article.

REFERENCES

1. M. J. Powell, *IEEE Trans. Electron Devices*, **ED-36**, 2753 (1989).
2. T. P. Brody, *IEEE Trans. Electron Devices*, **ED-31**, 1514 (1984).
3. K. C. Hsu, B. Y. Chen, H. T. Hsu, K. C. Wang, T. R. Yen, and H. L. Hwang, *Jpn. J. Appl. Phys.*, **33**, 639 (1994).
4. D. H. Kim, Y. B. Park, I. J. Lee and S. W. Rhee, *J. Elechem Soc.*, **143**, 2640 (1996).
5. X. Li, Y. B. Park, D. H. Kim, and S. W. Rhee, *Mater. Lett.*, **24**, 79 (1995).
6. A. H. Jayatissa, Y. Hatanaka, Y. Nakanishi, and T. Yamaguchi, *Jpn. J. Appl. Phys.*, **35**, 5687 (1996).
7. C. W. Lin and C. Y. Chang, *Jpn. J. Appl. Phys.*, **36**, 2032 (1997).
8. S. Ishihara, D. He, M. Nakata, and I. Shimizu, *Jpn. J. Appl. Phys.*, **32**, 1539 (1993).
9. K. Nomoto, Y. Urano, J. L. Guizot, G. Gangly, and A. Matsuda, *Jpn. J. Appl. Phys.*, **29**, L1372 (1990).
10. S. Veprek, *J. Chem. Phys.*, **56**, 952 (1972).
11. M. Otobe and S. Oda, *Jpn. J. Appl. Phys.*, **31**, 533 (1992).
12. N. Shibata, K. Fukuda, H. Ohtoshi, J. Hanna, S. Oda, and I. Shimizu, *Mater. Res. Soc. Symp. Proc.*, **95**, 225 (1987).
13. K. Nomoto, Y. Urano, J. L. Guizot, G. Ganguly, and A. Matsuda, *Jpn. J. Appl. Phys.*, **29**, L1372 (1990).
14. M. Otobe and S. Oda, *J. Non-Cryst. Solids*, **164-6**, 993 (1993).
15. Y. B. Park and S. W. Rhee, *Appl. Phys. Lett.*, **68**, 2219 (1996).
16. K. C. Wang and H. L. Hwang, *Mater. Res. Soc. Symp. Proc.*, **64**, 1024 (1994).
17. G. Lucovsky, D. V. Tsu, and R. J. Markunas, in *Handbook of Plasma Processing Technology*, S. M. Rossnagel, Editor, p. 392, Noyes Publications, Park Ridge, NJ (1990).
18. E. Stoffels, W. W. Stoffels, G. M. W. Koresen, and F. J. de Hoog, *J. Vac. Sci. Technol.*, **A14**, 56 (1996).
19. S. Mashima, A. Suzuki, G. Ganguly, Y. Toyoshima, and A. Matsuda, *Plasma Sources Sci. Technol.*, **2**, 23 (1993).
20. J. C. Knights, *J. Non-Cryst. Solids*, **35/36**, 289 (1981).
21. S. Harza, A. R. Middya, and S. Ray, *J. Appl. Phys.*, **78**, 581 (1995).
22. J. C. Knights and R. A. Lujan, *Appl. Phys. Lett.*, **35**, 244 (1979).
23. A. C. Fourd, D. L. Melville, and W. E. Spear, *Philos. Mag. B.*, **64**, 533 (1991).
24. D. V. Tsu, G. N. Parsons, and G. Lucovsky, *J. Vac. Sci. Technol.*, **A6**, 1849 (1988).
25. S. Veprek, Z. Iqbal, H. R. Oswald, and A. P. Webb. *J. Phys.*, **C14**, 295 (1981).
26. B. Drevillan, H. Shirai, and N. Layard, *J. Non-Cryst. Solids*, **164-6**, 989 (1993).
27. B. D. Cullity, *Elements of X-Ray Diffraction*, p. 102, Addison Wesley Publishers, Reading, MA (1978).
28. A. Matsuda, *J. Non-Cryst. Solid*, **59-60**, 767 (1983).
29. S. Yamasaki, H. Obeda, H. Okushi, and K. Tanaka, *Jpn. J. Appl. Phys.*, **21**, L539 (1982).
30. B. Drevillon, I. Solomon, and M. Fang, *Mater. Res. Soc. Symp. Proc.*, **283**, 455 (1993).
31. G. E. Jellison, J. M. Keefer, and L. Thornquistm, *Mater. Res. Soc. Symp. Proc.*, **283**, 561 (1993).
32. J. Tauc, in *Optical Properties of Solids*, F. Abeles, Editor, p. 277, North-Holland Publisher, Amsterdam (1972).
33. H. Kakinuma, S. Nishikawa, T. Watanabe, and K. Nihei, *J. Appl. Phys.*, **59**, 3110 (1986).
34. S. Yamasaki, *Philos. Mag.*, **B56**, 79 (1987).
35. B. Drevillon, J. M. Sietert, J. Huc, A. Lloret, G. de Rosny, and J. P. M. Schmitt, *Appl. Phys. Lett.*, **42**, 801 (1983).